

---

# Effects of Chromium on tribological properties of Ni<sub>3</sub>Al under dry sliding

CHEN Yanan, JIN Yunxue<sup>\*</sup>, NIU Muye, CHEN Hongmei

School of Materials Science and Engineering, Jiangsu University of Science and Technology,  
Zhenjiang 212003, China

**Keywords:** Ni<sub>3</sub>Al intermetallic, Cr content, Friction coefficient, Wear rate, Sliding wear performance

## ABSTRACT

Ni-25 at% Al intermetallic with different Cr contents was successfully produced by vacuum arc melting. Dry sliding tribological tests of the Ni<sub>3</sub>Al alloys were undertaken against Si<sub>3</sub>N<sub>4</sub>. Vickers hardness of the alloys was also measured. In order to study the wear mechanism, the worn surfaces of the alloys were examined by scanning electron microscopy (SEM). The results showed that hardness, friction coefficient and wear rate of the alloys increased with increasing of Cr contents. The Ni<sub>3</sub>Al-12Cr alloy obtained the best wear resistance properties compared to other three alloys. Besides, friction coefficient and wear rate declined with the increasing of loads. It was found that the dominant wear mechanism was oxidative wear and abrasive wear.

## INTRODUCTION

Intermetallic compounds have been developing rapidly with new material needed in the heavy duty diesel industry. View from both fundamental and practical, Ni<sub>3</sub>Al intermetallic compound has been extensively studied<sup>[1-8]</sup>. In the past few years, a lot of work has been concentrated on the research of the effect of alloying elements, mechanical properties, oxidation and corrosion. Ni<sub>3</sub>Al intermetallic compound depending on excellent comprehensive mechanical properties has been recognized as an alternative material for industrial application. A number of laboratory studies have indicated that Ni<sub>3</sub>Al alloys have significant potential in wear-critical applications<sup>[9-14]</sup>. The unique performance of Ni<sub>3</sub>Al leads to various tribomaterials developments<sup>[15-16]</sup>

Most studies focused on high temperature properties, however, Ni<sub>3</sub>Al also possess certain properties which make them potential for room temperature applications. According to the references [17-20], Cr additions to Ni<sub>3</sub>Al that existed as a solution have been reported about 8 at% Cr shows great ability of suppressing the oxygen embrittlement of Ni<sub>3</sub>Al alloys at intermediate temperatures. P. Adeva et al.<sup>[21]</sup> investigated the microstructural evolution of a powder metallurgy (PM) Ni<sub>3</sub>Al-8Cr (at%) alloy reinforced with Cr particles. In this paper, since Cr particles will be located at the original particle boundaries of the Ni<sub>3</sub>Al powder, Cr reinforcing particles may act as a chromium supply source during deformation, promoting the formation of a protective oxide film to shut out the gaseous oxygen entering through the particle and grain boundaries. The present study is to investigate tribological properties of Ni-25at% Al intermetallic compound with different Cr content. This experiment researched the effects of chromium on tribological properties of Ni<sub>3</sub>Al under room- temperature dry sliding.

## 1 EXPERIMENT METHODS

The initial materials were commercial Al, Ni and Cr (Ni-to-Al atomic ratio is 3:1). Ni<sub>3</sub>Al–X Cr (X denote the alloy with at% content of Cr) alloys were synthesized by the high temperature electric arc furnace melting. The chemical composition of the alloys is shown in Table 1. Experimental specimens were cut by a wire-electro-discharging.

Before tribological tests, Ni<sub>3</sub>Al phase were identified by using X-ray (XRD, Rigaku ME510-FM2), scanning electron microscope (SEM, JEOL-5410), and energy dispersive spectrometry (EDS). X-ray diffractometer at a scanning speed of 6 °/min and a scanning range from 20 ° to 90 ° used a copper target and an applied voltage and current of 30 KV and 20 mA respectively. The morphologies of the samples were studied by using scanning electron microscopy (SEM, JOEL JSM-6600). The Vickers hardness of the Ni<sub>3</sub>Al–X Cr alloys were measured by a Vickers indentation technique with an endurance time of 10 s, the average of nine repeat tests was given. Compression properties were evaluated by using an UTM5205X testing system with a loading speed of 1.2 mm/min on samples with dimension of Φ5 mm × 10 mm. The wear test specimens were cut into the dimension of Φ10 mm × 2.5 mm, and the surface of the specimens were polished. In order to reduce the experiment errors and keep the surface clean, the ball and specimen were ultrasonically cleaned using ethyl alcohol, and dried with hot air before wear experiments. The wear behavior was measured by a HT-1000 ball-on-disk high-temperature tribometer.

The counterpart ball was the commercial Si<sub>3</sub>N<sub>4</sub> ball with diameter of 6 mm, the Ni<sub>3</sub>Al–X Cr alloy as a disk. The sliding speed of 10.4 cm/s was selected as a constant value by adjusting the rotation speed (200 r/min) of the disk and the diameter (diameter 5 mm) of wear track. Each tribological test lasted 30 min at applied loads ranged from 5 N to 20 N. The cross-section profile of worn surface was measured using a surface profilometer. The wear volume was determined as  $V = AL$ , where A was the cross-section area of worn scar and the values were averages of four replicates, and L was the perimeter of the worn scar. The volumetric wear rate was evaluated using Eq. (1).

$$W = \frac{V}{FS} \quad (1)$$

where V was the volume worn away in mm<sup>3</sup>, F was the normal load in N, S was the sliding distance in meter, and W was wear rate in mm<sup>3</sup>/N m.

Table 1 Compositions and mechanical properties of the Ni<sub>3</sub>Al-X Cr alloys

Compound	Compositions (at%)	Hardness (HV)	Compressive strength (MPa)
Ni <sub>3</sub> Al	Ni <sub>3</sub> Al	201	1854
Ni <sub>3</sub> Al-4Cr	Ni <sub>3</sub> Al+4%Cr	246	1968
Ni <sub>3</sub> Al-8Cr	Ni <sub>3</sub> Al+8%Cr	315	2143
Ni <sub>3</sub> Al-12Cr	Ni <sub>3</sub> Al+12%Cr	357	2197

## 2 RESULTS AND DISCUSSION

Fig.1 shows the XRD patterns of Ni<sub>3</sub>Al–X Cr alloys. It was noted that the material without Cr element only formed single Ni<sub>3</sub>Al phase, and (100), (110) and (211) crystal indices were ordered Ni<sub>3</sub>Al

phase<sup>[22]</sup>. With the increasing of Cr content, there was no chromium compound in the XRD patterns, beside, the peak of Ni<sub>3</sub>Al continuously shifted to the left. If it exhibited chromium compounds, the peak of Ni<sub>3</sub>Al would slide to the right that was the direction of the lattice distortion decreasing<sup>[23]</sup>. As a result, Cr element existed in Ni<sub>3</sub>Al alloy in the form of solid solution resulting in the lattice distortion continuously increasing.

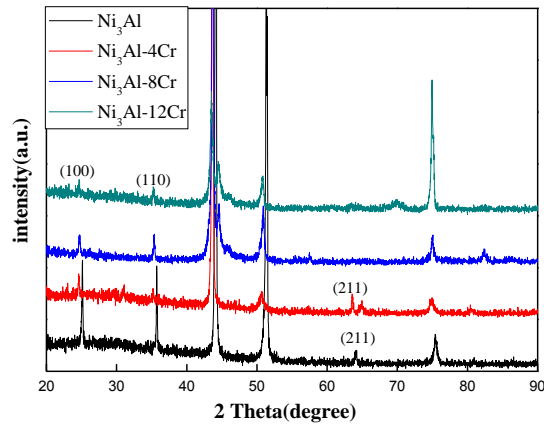
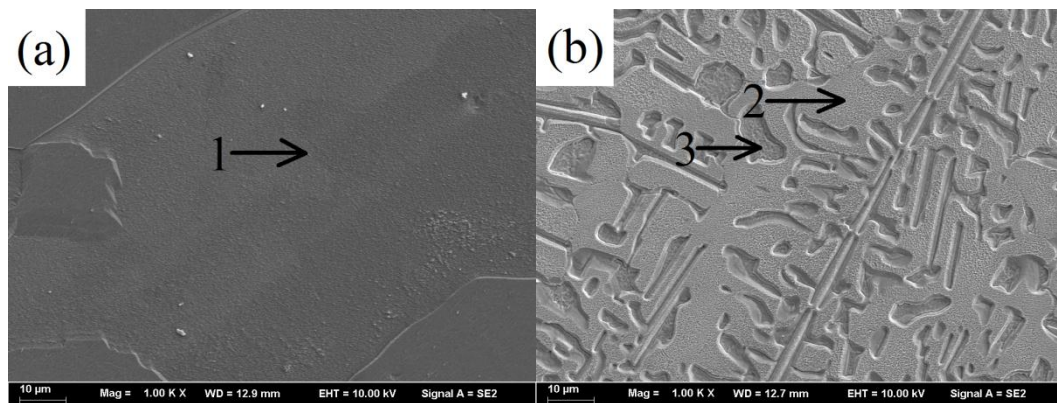


Fig.1 XRD patterns of Ni<sub>3</sub>Al alloys with different Cr contents

Fig.2 shows the microstructures of Ni<sub>3</sub>Al-X Cr alloys. There was no apparently dendrite and interdendritic in pure Ni<sub>3</sub>Al intermetallic compound (shown in Fig.2 (a)). However, dendrite and interdendritic were obtained in other three alloys, at the same time, volume fraction of interdendritic regions decreased evidently with the increasing of Cr content. According to the EDS results (shown in Table 2), Cr content in dendrite was a little higher than that in interdendritic (even numbers denote dendrite, odd numbers denote interdendritic, except number 1). Besides, there was no difference between the hardness of dendrite and interdendritic.



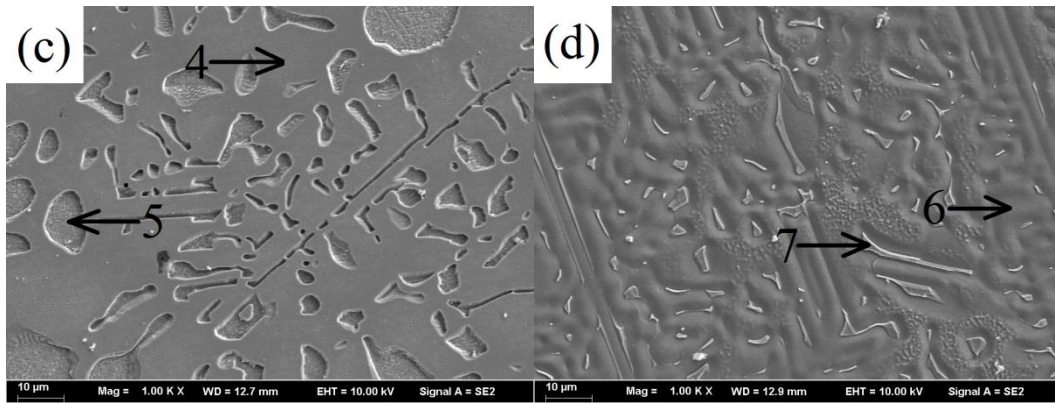


Fig.2 The SEM micrographs of  $\text{Ni}_3\text{Al}$  alloys with different Cr contents  
(a)  $\text{Ni}_3\text{Al}$ , (b)  $\text{Ni}_3\text{Al-4Cr}$ , (c)  $\text{Ni}_3\text{Al-8Cr}$ , (d)  $\text{Ni}_3\text{Al-12Cr}$

Table 2 Chemical composition of  $\text{Ni}_3\text{Al-X Cr}$  alloys in atomic percentage

Area	Elements		
	Ni	Al	Cr
1	74.03	25.97	-
2	79.00	16.14	4.86
3	71.33	26.49	2.17
4	76.69	13.96	9.36
5	68.45	25.17	6.38
6	71.92	15.64	12.43
7	67.58	24.65	7.78

The variation of friction coefficients of  $\text{Ni}_3\text{Al-X Cr}$  alloys with loads at a sliding speed of 10.4 cm/s under air condition is given in Fig.3. It was clear that friction coefficients of each material decreased with the increase of loads. It could be found that the friction coefficients of the  $\text{Ni}_3\text{Al-X Cr}$  alloys fluctuated between 0.4 and 0.6 and continued to decrease as the load increasing. Furthermore, under the same loading condition, with the increasing of Cr contents, friction coefficients of alloys declined, which because the extended hardness (shown in Table 1) reduced contact areas between ball and disk with the increase of Cr contents.

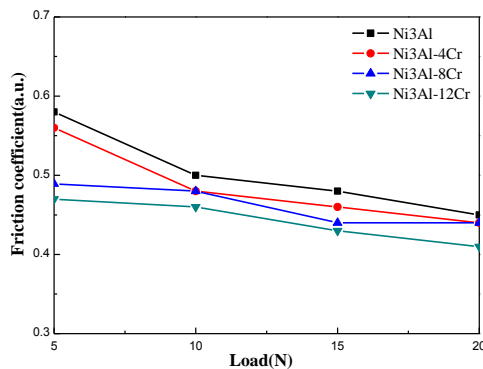


Fig.3 Variations of friction coefficients the  $\text{Ni}_3\text{Al-XCr}$  alloys under different loads

Fig.4 shows the profiles of wear tracks of Ni<sub>3</sub>Al-XCr alloys with 10N load at sliding friction. Obviously, with the increasing of Cr contents, the width and depth of the worn track reduced. The friction coefficient of materials under dry sliding friction conditions could be expressed by the following formula (2), where  $\mu$  was the friction coefficient, S was the shearing stress, A was the apparent contact area and W was the normal load<sup>[24,25]</sup>.

$$\mu = \frac{SA}{W} \quad (2)$$

Therefore, under the same load, the apparent contact area was decreasing as the amount of Cr increased due to the hardness increased as the amount of Cr increased (Shown in Table 1). So the friction coefficient of Ni<sub>3</sub>Al-12Cr was the smallest.

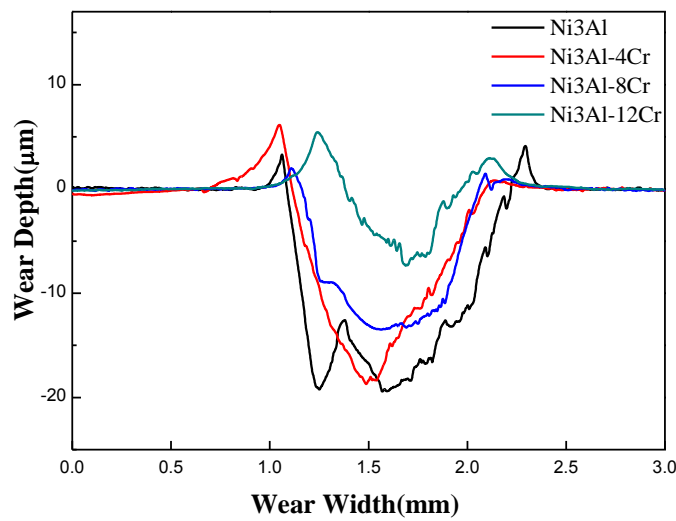


Fig.4 The profiles of wear tracks of Ni<sub>3</sub>Al alloys with 10N load at sliding friction

Fig.5 shows the variations of wear rates of the Ni<sub>3</sub>Al-XCr alloys under different loads. These results verified that the increasing in loads resulted in decrease in wear rate. Under the same loading condition, the wear rate of test materials decreased with the increasing of Cr content. Ni<sub>3</sub>Al alloy without Cr showed the highest wear rate than other materials with the loads increasing, ranging from  $2.1 \times 10^{-6} \text{ mm}^3/\text{N m}$  to  $9.5 \times 10^{-7} \text{ mm}^3/\text{N m}$ . And Ni<sub>3</sub>Al-12Cr exhibited the minimum wear rate ranging from  $1.7 \times 10^{-6} \text{ mm}^3/\text{N m}$  to  $8.4 \times 10^{-7} \text{ mm}^3/\text{N m}$ . It indicated that the moderate Cr additions to Ni<sub>3</sub>Al alloy improved the load-bearing ability (shown in Table 1) and anti-wear properties under dry sliding friction.

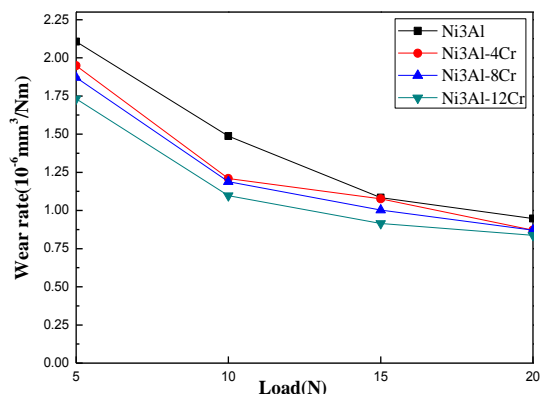


Fig.5 Variations of friction coefficients the Ni<sub>3</sub>Al-XCr alloys under different loads

Fig.6 shows the micro morphologies of the worn surfaces of Ni<sub>3</sub>Al-X Cr alloys with 10N load at sliding friction. The micro morphologies of the worn surfaces of all four materials were apparently covered by grooves and cracks. As can be seen in Fig.6(a)-(d), the worn surface of the Ni<sub>3</sub>Al alloy possessed obvious grooves and cracks compared to the other three materials. When compared to Ni<sub>3</sub>Al alloy, the cracks of Ni<sub>3</sub>Al-4Cr were significantly reduced. It was obvious that there were shallow grooves and almost no cracks in Ni<sub>3</sub>Al-8Cr alloy. It was worth noting that Ni<sub>3</sub>Al-12Cr exhibited not only least grooves but also least cracks than that of other materials. Combining with Table 1, it meant an increase load-bearing ability in Ni<sub>3</sub>Al-12Cr owing to the high hardness, which was also confirmed with the compressive strength.

The distribution of different elements on worn surface of each area was determined by EDS (shown in Table 3). The EDS analysis of the wear track formed on the worn sample showed that wear tracks contain high oxygen while there was no oxygen before wear test (shown in Table 2). It was possible to claim that the oxides formed on the surface of test materials and the presence of oxygen in rubbing surface confirms the formation of nickel oxide and aluminum oxide or chromium oxide; and the tiny amounts Si element came from Si<sub>3</sub>N<sub>4</sub> ceramic ball. Although each area contained O, it was worth nothing that oxygen content in the areas of even numbers (shown in Fig.6 II,IV,VI,VIII) were no wear off is higher than that of odd numbers (shown in Fig.6 I,III,V,VII). It signified that the temperature was increased so that oxidation of the alloys occurred during the sliding experiment. Another important feature was the formation of cracks/flaws. These cracks eventually led to material decohesion/detachment due to plastic deformation under cyclic forces. Stott<sup>[26]</sup> has claimed that the oxidation layer occurring on the surface decreases the wear rate. Hence, considering the analysis above, it could make a conclusion that the wear mechanism contained abrasive wear and oxidative wear.

The addition of Cr increased the hardness and compressibility of the material (shown in Table 1); and there was no difference between the hardness of dendrite and interdendritic. Based on above analysis, Ni<sub>3</sub>Al-12Cr possessed high load-bearing ability and excellent anti-wear performance.

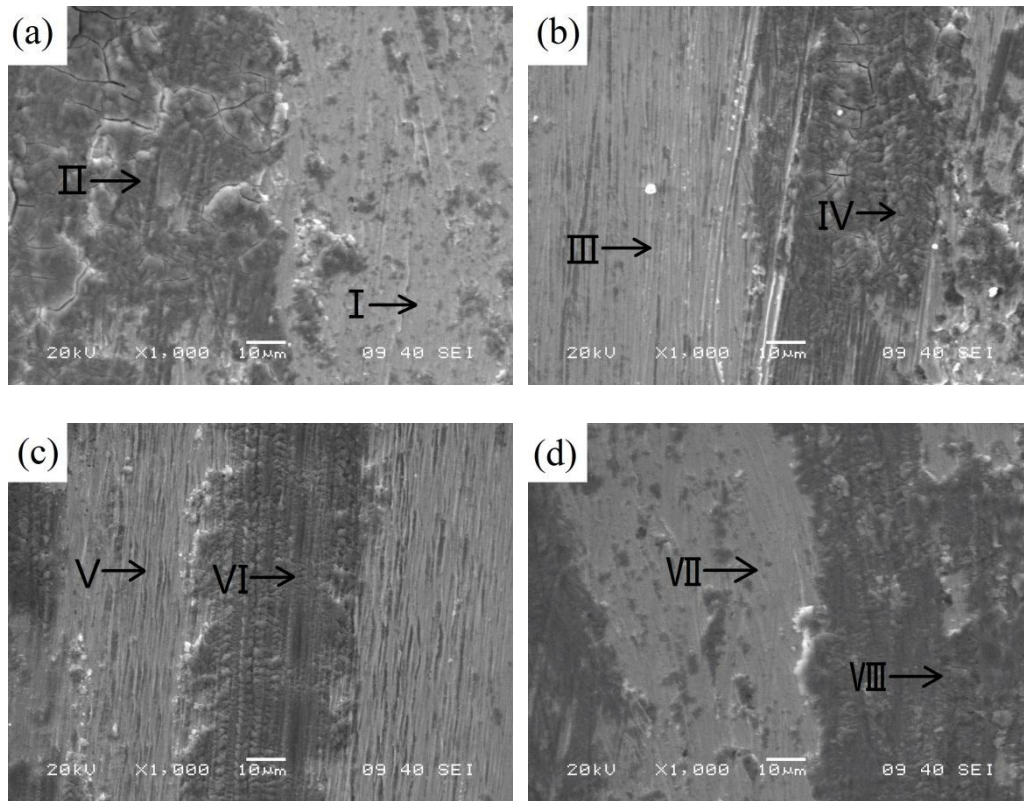


Fig.6 The morphologies of the worn surfaces of  $Ni_3Al-X$  Cr alloy with 10N load  
 (a) $Ni_3Al$ , (b) $Ni_3Al-4Cr$ , (c) $Ni_3Al-8Cr$ , (d) $Ni_3Al-12Cr$

Table 3 Compositions of worn surface of each area (at%)

Area	Elements				
	Ni	Al	Cr	O	Si
I	66.44	21.46	-	12.10	-
II	39.13	13.15	-	47.71	-
III	65.57	20.36	4.63	9.43	-
IV	28.94	8.03	1.65	58.45	2.93
V	56.81	17.95	6.77	18.47	-
VI	30.60	9.10	3.72	54.07	2.51
VII	53.58	22.89	8.45	15.08	-
VIII	27.97	9.94	5.36	55.68	1.05

The morphologies of the worn surfaces of the  $Ni_3Al-12Cr$  under different load are given in Fig.6 (d) and Fig.7 (a)-(c). When test materials ran for 5 N (Fig.7 (a)), grooves and cracks were visible. With the increasing in loads, small grinding debris appeared on the worn surface; and grooves and cracks were not obvious. When the applied loads increased to 20N (Fig.7 (c)), abrasion area distributes fine size debris, and there was no crack. Debris was adhered to worn surface and a film of wear debris was formed on the worn surfaces in the sliding owing to the high temperature on the worn surfaces<sup>[27]</sup>. In this case, the worn surfaces were protected from abrasion of debris by the film. At the same time, it also confirmed that the friction coefficient was smaller under high loads (shown in Fig.3).

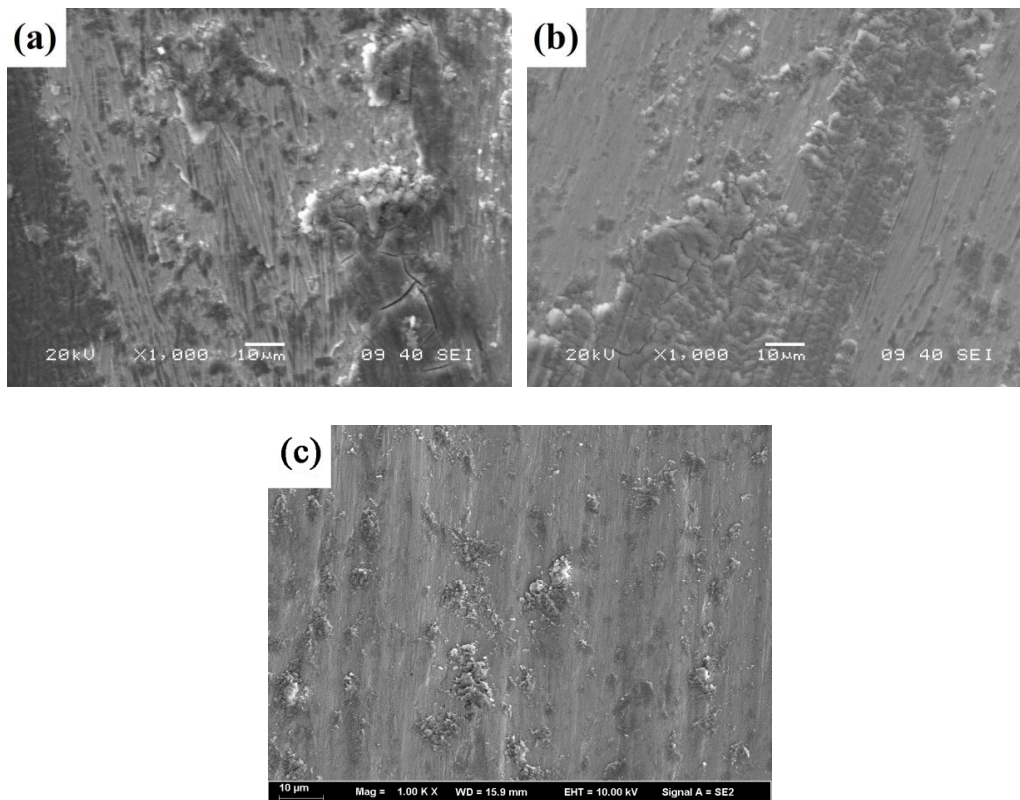


Fig.7 The morphologies of the worn surfaces of the Ni<sub>3</sub>Al-12Cr under different load  
(a) 5N, (b)15N, (c) 20N

### 3 CONCLUSIONS

Effects of chromium added on tribological properties of Ni<sub>3</sub>Al under dry sliding were investigated. The following results can be drawn from the present study:

(1) Ni<sub>3</sub>Al alloys were successfully produced by vacuum arc melting. Cr element existed in Ni<sub>3</sub>Al alloy in the form of solid solution. Hardness and compressive strength of Ni<sub>3</sub>Al alloys increased with increasing of Cr added content. Ni<sub>3</sub>Al-12Cr possessed the highest Vickers hardness and compressive strength.

(2) Under the same loads, the response of the friction coefficients and the wear rates of the four alloys to Cr content were differentiable. The friction coefficient and wear rate of Ni<sub>3</sub>Al-12Cr both declined compared with other three materials.

(3) With the increase in loads, the friction coefficient and wear rate of each alloys decreased.

(4) The dominant wear mechanism had been found to be oxidative wear and abrasive wear due to the high oxygen and grooves concentration on the worn track.

### REFERENCES

- [1] Niu MY, Bi QL, Kong LQ, Yang J, Liu WM, A study of Ni<sub>3</sub>Si-based composite coating fabricated by self-propagating high temperature synthesis casting route, *Surface & coatings*



- 
- technology*, 205, 2011, pp. 4249–4253.
- [2] Liu CT, White CL, Dynamic embrittlement of boron-doped Ni3Al alloys at 600 °C, *Acta Metall*, 35, 1987, pp. 643–649.
- [3] Czepe T, Wierzbinski S, Structure and mechanical properties of NiAl and Ni3Al-based alloys, *International Journal of Mechanical Sciences*, 42, 2000, pp.1499–1518.
- [4] Sikka VK, Deevi SC, Viswanathan S, Swindeman RW, Santella ML, Advances in processing of Ni3Al-based intermetallics and applications, *Intermetallics*, 8, 2000, pp. 1329–1337.
- [5] Lee WH. Oxidation and sulfidation of Ni3Al, *Materials Chemistry and Physics*, 76, 2002, pp. 26–37.
- [6] Pérez P, González-Carrasco JL, Adeva P, The effect of Cr implantation on the isothermal–oxidation behavior of a Ni3Al PM alloy, *Oxidation of Metals*, 51, 1999, pp. 273–289.
- [7] Blau PJ, DeVore CE, Sliding friction and wear behaviour of several nickel aluminide alloys under dry and lubricated conditions, *Tribology International*, 23, 1990, pp.226–234.
- [8] Ricker RE, Origins of the aqueous corrosion and stress corrosion cracking behavior of ductile nickel aluminide, *Materials Science and Engineering: A*, 198, 1995, pp. 231–238.
- [9] Zhu S, Bi Q, Yang J, Qiao Z, Ma J, Li F, Yin B, Liu W, Tribological behavior of Ni3Al alloy at dry friction and under sea water environment, *Tribology International*, 75, 2014, pp. 24–30.
- [10] Karin G, Luo H, Feng D, Li C, Ni3Al-based intermetallic alloys as a new type of high-temperature and wear-resistant materials. *Journal of Iron and Steel Research*, 14, 2007, pp. 21–25.
- [11] Deevi S.C, Sikka V.K, Nickel and iron aluminides: An overview on properties, processing, and applications, *Intermetallics*, 4, 1996, pp. 357–375.
- [12] P.J. Blau, C.E. DeVore, Proceedings of the 1989 Wear of Materials Conference, *American Society of Mechanical Engineers*, 1989, pp. 305.
- [13] P.J. Blau, C.E. DeVore, Sliding friction and wear behaviour of several nickel aluminide alloys under dry and lubricated conditions *Tribology International*, 23, 1990, pp. 226-234.
- [14] M. Johnson, D.E. Mikkola, P.A. March, R.N. Wright, The resistance of nickel and iron aluminides to cavitation erosion and abrasive wear, *Wear*, 140, 1990, pp. 279-289.
- [15] Zhu SY, Bi QL, Yang J, Liu WM, Xue QJ, Ni3Al matrix high temperature selflubricating Composites, *Tribology International*, 44, 2011, pp. 445–453.
- [16] Zhang XH, Yang J, Ma JQ, Bi QL, Cheng J, Liang YM, et al, Microstructures and mechanical Properties of Fe–28Al–5Cr/TiC composites produced by hotpressing sintering, *Materials Science and Engineering: A*, 528, 2011, pp. 6819–6824.
- [17] Liu CT, White CL, Dynamic embrittlement of boron-doped Ni3Al alloys at 600°C, *Acta Metallurgica*, 35, 1987, pp. 643–649.
- [18] Lapin J, Effect of ageing on the microstructure and mechanical behaviour of a directionally solidified Ni3Al-based alloy, *Intermetallics*, 5, 1997, pp. 615–624.
- [19] Sikka VK, Deevi SC, Viswanathan S, Swindeman RW, Santella ML, Advances in processing of Ni3Al-based intermetallics and applications, *Intermetallics*, 8, 2000, pp. 1329–1337.
- [20] Czepe T, Wierzbinski S, Structure and mechanical properties of NiAl and Ni3Al-based alloys, *International Journal of Mechanical Sciences*, 42, 2000, pp. 1499–1518.
- [21] J. Garcí'a Barriocanal, P. Pe´rez, G. Garce´s, P. Adeva, Microstructure and mechanical properties of Ni3Al base alloy reinforced with Cr particles produced by powder metallurgy,

- Intermetallics*, 14, 2006, pp. 456–463.
- [22] M. Pal, S.K. Pradhan, P. Bose, A. Datta, D. Chakravorty, Order–disorder transition in nanocrystalline Ni<sub>3</sub>Al prepared by a chemical route, *Physica E: Low-dimensional Systems and Nanostructures*, 31, 2006, pp. 224 – 227.
- [23] Z.Y. Rao, X. Wang, J. Zhu, X.H. Chen, L. Wang, J.J. Si, Y.D. Wu, X.D. Hui, Affordable FeCrNiMnCu high entropy alloys with excellent comprehensive tensile properties, *Intermetallics*, 77, 2016, pp. 23-33.
- [24] Y. Wan, W. Liu, Q. Xue, Effects of diol compounds on the friction and wear of aluminum alloy in a lubricated aluminum-on-steel contact, *Wear*, 193, 1996, pp. 99–104.
- [25] Peter J. Blau, *Metals Handbook*, 10th Edition, The Materials Information Society, USA, 1990.
- [26] Stott FH, The role of oxidation in the wear of alloys. *Tribology International*, 31, 1998, pp. 61–71.
- [27] F.P. Bowden, D. Tabor, *The Friction and Lubrication of Solids*, Part 2, Oxford University Press, Oxford, 1954.